ciency in the Aging Male（PADAM）という概念も提唱されている．閉経後の女性では，エストロゲンの産生が著しく低下しているせいか，エストロゲン濃度よりもむしろアンドロゲン濃度の方が閉経後以降の老化には関係するとされる．男性と同様，低アンドロゲン血症が骨粗鬆症，肥満，高脂血症の発症と関連したことが報告されている．

2 テストステロンの作用とアンドロゲン受容体（AR）の役割

テストステロンは，核内受容体であるARに作用して標的遺伝子の転写を調節する（図4）．テストステロンはさらに，5α-還元酵素により活性の強いdehydrotestosterone（DHT）に変換されてARに作用する，あるいはアロマターゼによりエストラジオールに変換されてERに作用する経路も存在することにも注意を要する．

ARの役割を解析する目的で作製されたAR欠損マウスのオスは外見上メス型で不妊である[2]．また，高代謝回転型の骨量減少を示し，AR機能が正常な骨形成に必須であることが証明された．さらに，AR欠損マウスのオスは晩発性の肥満を呈し，白色脂肪の顕著な蓄積がみられた．このように，ヒトでも報告されているテストステロンの骨量維持効果や抗肥満効果の少なくとも一部はARを介すると考えられる．一方，LDL受容体欠損マウスに高コレステロール食を負荷した研究[3]では，粥状硬化の程度は精巣摘出により増加し，テストステロン投与で減少した．しかし，テストステロンによる抑制効果はアロマターゼ阻害薬の同時投与で消失したことから，むしろ変換されたエストラジオールの効果によるものと考えられる．

3 DHEAの作用とその機序

DHEAはステロイド生合成系の比較的上流に位置する（図6）．DHEA独自の受容体は同定されていないため，代謝されてテストステロンとして作用を発揮すると考えられている．実際DHEAの作用はテストステロンと類似した部分があり，アンドロゲンに分類されるが，さらにアロマターゼにより変換されてエストロゲンとしての作用も発揮しうる．その意味で男女

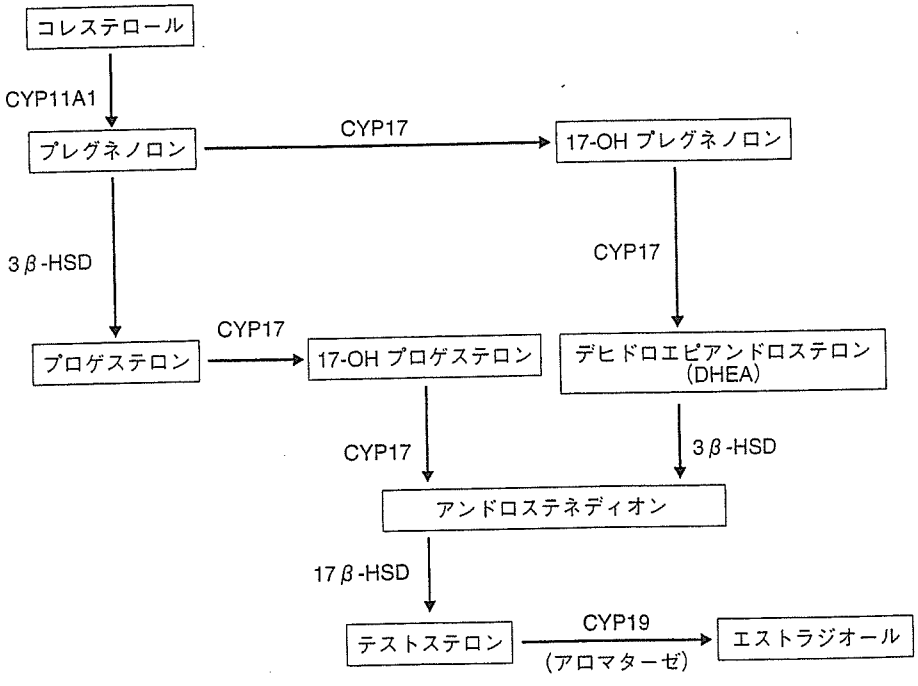

図6 性ステロイド生合成系

双方に生理作用を有することは明らかで，抗老化ホルモンとして注目される所以である．

GH/IGF-1

GHは脳下垂体から分泌され，IGF-1の産生を介して，肝，骨，筋肉，性腺など多くの臓器に対して細胞増殖，タンパク合成作用を発揮する．GHの分泌は視床下部から分泌されるGH放出ホルモン（GH-RH）とソマトスタチンにより調節されているが，最近発見された消化管ホルモンのグレリンもGH分泌に作用することがわかり注目されている．また，性ホルモンもGH分泌調節に関与することが報告されている．

GH分泌能も血中IGF-1濃度も加齢に伴って低下する．GH欠乏では成長障害がみられる，逆にいえばGH/IGF-1系が正常な体の成長に必須であることから，GH/IGF-1は老化にも関連するのではないかと考えられてきた．実際，一部ではアンチエイジング目的でGH注射が行われている．また，線虫や昆虫の実験ではIGF-1やインスリンシグナルの活性化により寿命が延長することが証明されている．

一方，よりヒトに近い種として検討されたマウスの実験では，全く逆の結果が得られている．自然発生した変異や遺伝子改変マウスの解析では，GH分泌，GH受容体，IGF受容体などGH/IGF-1系に障害があると，いずれの系統でもマウスの寿命が1.5倍から2倍にまで延長した[4]．そのメカニズムとしては，代謝および酸化ストレスの低下，発ガン性の減少などが提起されている．ヒトでも，GH分泌不全やGH/IGF-1系の遺伝子変異があると低身長で長生きしたこと，GH分泌過剰では寿命が短いことなどが報告されており，あながちマウスだけの現象とはいえないようである．長寿とアンチエイジングとは同義ではないが，今後の研究によりGH/IGF-1系と老化の関係を明確にする必要がある．

文　献

1) Sudhir K,et al：Premature coronary artery disease associated with a disruptive mutation in the estrogen receptor gene in a man. Circulation 1997；96：3774-3777.
2) Kawano H, et al：Suppressive function of androgen receptor in bone resorption. Proc Natl Acad Sci U S A 2003：100：9416-9421.
3) Nathan L, et al：Testosterone inhibits early atherogenesis by conversion to estradiol：critical role of aromatase. Proc Natl Acad Sci U S A 2001；98：3589-3593.
4) Bartke A：Minireview：role of the growth hormone/insulin-like growth factor system in mammalian aging. Endocrinology 2005：146：3718-3723.

実　践　編

機能からみたエイジングの予防と治療

第3章

4　ホルモン

東京大学大学院医学系研究科加齢医学　秋下雅弘

はじめに

加齢に伴い多くのホルモンの血中濃度が低下し，やはり加齢現象である老化度の進行や疾患の発生の原因となっている可能性がある．しかし，女性の閉経のような急激な変化はむしろまれであり，ホルモンの低下も老化のプロセスも通常は緩徐に進む．したがって，ホルモンの経年的低下と老化との関連は加齢という交絡因子を排除して解析する必要がある．そのような臨床研究の結果，男性ホルモンのテストステロン，副腎由来アンドロゲンのDehydroepiandrosterone（DHEA），下垂体系の成長ホルモン（Growth hormone：GH）/インスリン様成長因子（Insulin-like growth factor：IGF）に関しては老化との関連を示す多くの報告がみられる．同時に，低下したホルモンを補充することで老化の進行や老年疾患の発症を遅らせることができるかどうかも閉経後女性に対するエストロゲン補充療法の大規模臨床試験を始め，様々な種類の研究で検討されている．本稿では，上記4種類のホルモンについて，ホルモン低下と老化および疾患との関係，ホルモン補充療法による介入効果を解説する．

エストロゲン

1　閉経と疾患

更年期以前の女性は概して男性より健康で，健康診断で指摘される生活習慣病関連の異常項目も少ない．ところが50歳前後の更年期から，冷えや火照りなどの血管運動神経症状，不眠やうつなどの精神症状が更年期障害として頻繁に認められるようになる．同時に，LDLコレステロールの増加を主体とした高脂血症，高代謝回転型の骨量減少，高血圧，肥満など生活習慣病の頻度が顕著に増加する．これらの結果，老年期には骨粗鬆症，心筋梗塞や脳梗塞などの動脈硬化性疾患，さらにアルツハイマー病の発生が増加する．

2　エストロゲン補充療法の効果

エストロゲン補充療法は，実際には子宮がんの増加を抑える目的でプロゲスチン製剤を併用することが多いので，ホルモン補充療法（Hormone Replacement Therapy：HRT）とよばれる．わが国では2%程度の閉経後女性が実施しているに過ぎないが，北米では40%，欧州や韓国，台湾でも10%以上もの女性が行っている．

HRTの短期効果として，更年期障害，萎縮性膣炎，高コレステロール血症の改善があげられる．一方，長期効果については，Women's Health Initiative（WHI）に代表される大規模臨床試験の結果が予想外に悪く，HRTの適応について議論となっている．WHIでは，閉経後女性を対象に結合型エストロゲンと酢酸メドロキシプロゲステロン併用によるHRTの有用性を検討した．平均5.2年間の追跡期間中，HRTにより乳がん，静脈血栓症・肺塞栓症のみならず，冠動脈疾患は1.29倍に，脳卒中も1.41倍に増加してしまった（図1）．それまで証明されていなかった（おそらく骨粗鬆症に対する効果を介した）骨折と大腸がんの減少を認めたものの，総合評価として閉経後女性にHRTは好ましくない治療であるとされた．その

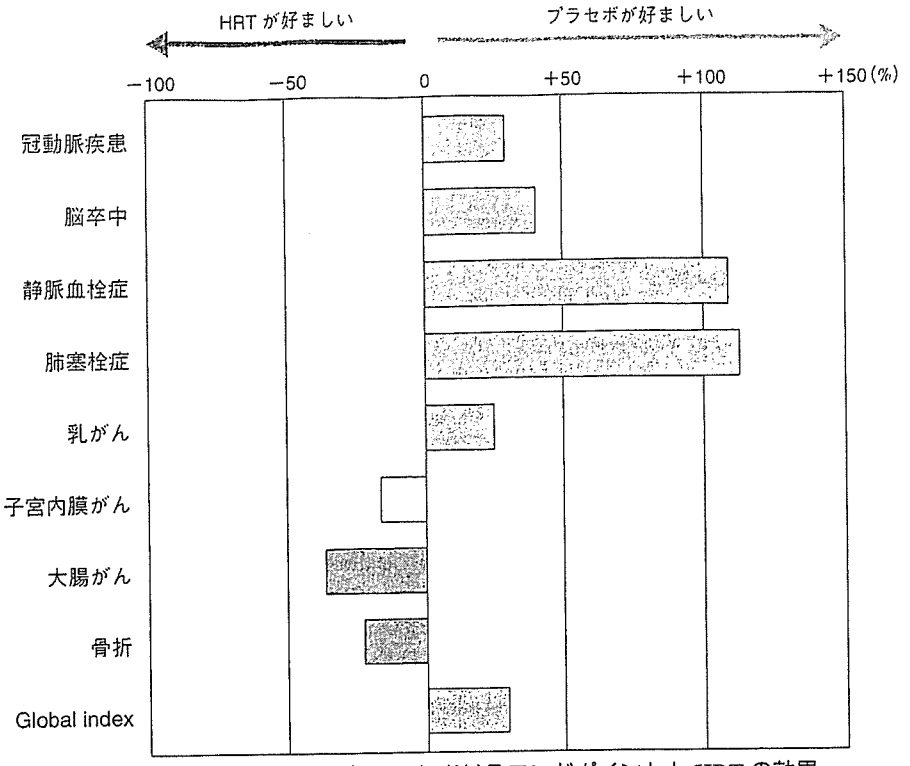

図1　Women's Health Initiative におけるエンドポイントと HRT の効果
(Rossouw JE, et al. Risks and benefits of estrogen plus progestin in healthy postmenopausal women: principal results From the Women's Health Initiative randomized controlled trial. JAMA 2002；288：321-33 より引用)

表1　心血管疾患に関係するエストロゲンの作用

	好ましいもの	好ましくないもの
脂質	LDL-C 減少 HDL-C 増加	トリグリセリド増加 small, dense LDL 増加
凝固・線溶系	PAI-1 低下 フィブリノゲン低下	プロトロンビンフラグメント増加 Ⅶ因子増加 アンチトロンビンⅢ低下
炎症 / 接着	接着分子低下	CRP 増加
血圧 / 心血管	ACE 活性低下 内皮依存性血管拡張作用 NO 増加 ET-1 低下，PGI_2 増加 平滑筋細胞遊走・増殖抑制	アンジオテンシノーゲン増加

後，エストロゲン単独療法の結果も報告されたが，やはり心疾患を減らす効果はなく，認知症に対する効果も否定された．

結局，エストロゲンは心血管系に対しても好ましい作用と好ましくない作用を有し（表1），状況によって悪い作用が前面に出てしまうと考えられる．また，プロゲステロン併用，用量の多さ，対象が高齢者であったことなども WHI の結果に影響しているとされる．これらの点を考慮し，現時点でも，喫煙，肥満，糖尿病，高血圧，心血管疾患の既往，血栓性疾患，がんの既往・素因を有していない閉経後間もない女性では，十分なインフォームドコンセントのもとに HRT

を実施することに大きな問題はないと思われる．ただし，有害作用予防のために，半量投与および貼付剤によるHRTを選択することが望ましい．

テストステロンとDHEA

1 男性におけるアンドロゲン低下と疾患

日本泌尿器科学会の調査[1]では，遊離テストステロン濃度は20歳代以降10年毎に1.6 pg/ml（9.2%）低下するとされる．このようなテストステロンの経年的低下と関連して多くの老年疾患が発症することが報告されている．

テストステロンと骨粗鬆症との関係は古くから指摘されているが，テストステロンからアロマターゼにより変換されるエストラジオールの影響も強いとされる．テストステロン補充療法の骨量に対する効果についても賛否あるが，Snyderらのプラセボ対照二重盲検比較試験[2]では，若年成人平均より1SD以上のテストステロン低下を示した高齢男性に貼付剤によるテストステロン補充療法を行ったところ，群全体ではプラセボに比べて有意な骨量増加を認めなかったが，治療前のテストステロン濃度が低い場合には骨量が増加した．Snyderらは同様の研究で，体脂肪の有意な減少と筋肉量の増加を示している．

動脈硬化とアンドロゲンについては，いくつかの症例対照比較試験で，テストステロンやDHEAの低値が高齢男性の脳梗塞および心筋梗塞の発症，冠動脈狭窄度と関係することが報告されている．また，40～70歳の男性1,709名を対象としたMassachusetts Male Aging Studyという横断疫学研究では，遊離テストステロン低値およびDHEA-sulfate（DHEA-S）の低値は独立した心疾患の危険因子であった（図2）．一方，アンドロゲン低下に伴う代謝性変化として，HDLコレステロール低下，トリグリセリド増加といった脂質

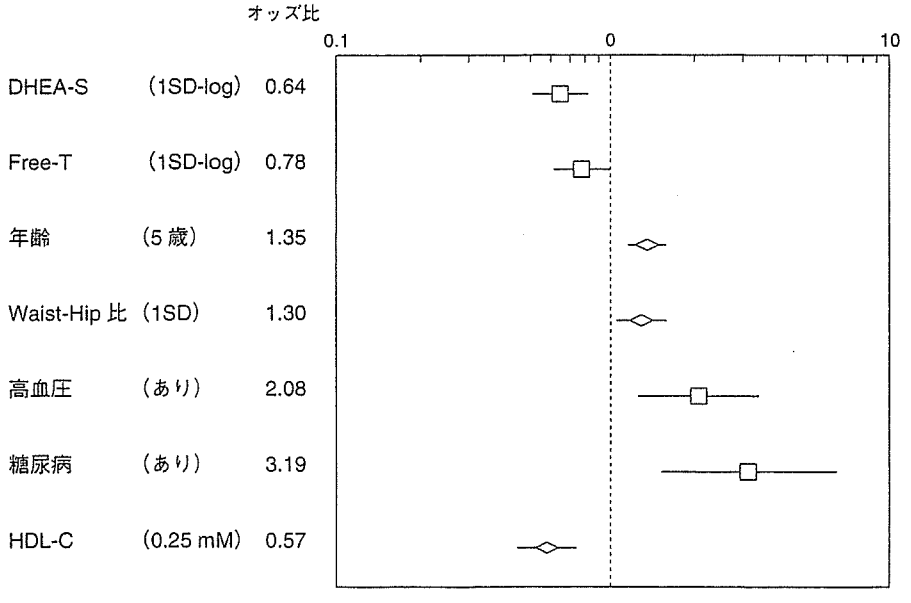

DHEA-S, Dehydroepiandrosterone-sulfate; Free-T, 遊離テストステロン；
HDL-C, HDLコレステロール

図2 中高年男性におけるアンドロゲン濃度と心疾患の発症
Massachusetts Male Aging Study，40-70歳の男性1,709名の追跡研究
（Feldman HA, et al：Low dehydroepiandrosterone sulfate and heart disease in middle-agedmen：crosssectional results from the Massachusetts Male Aging Study. Ann Epidemiol 1998；8：217-228より引用）

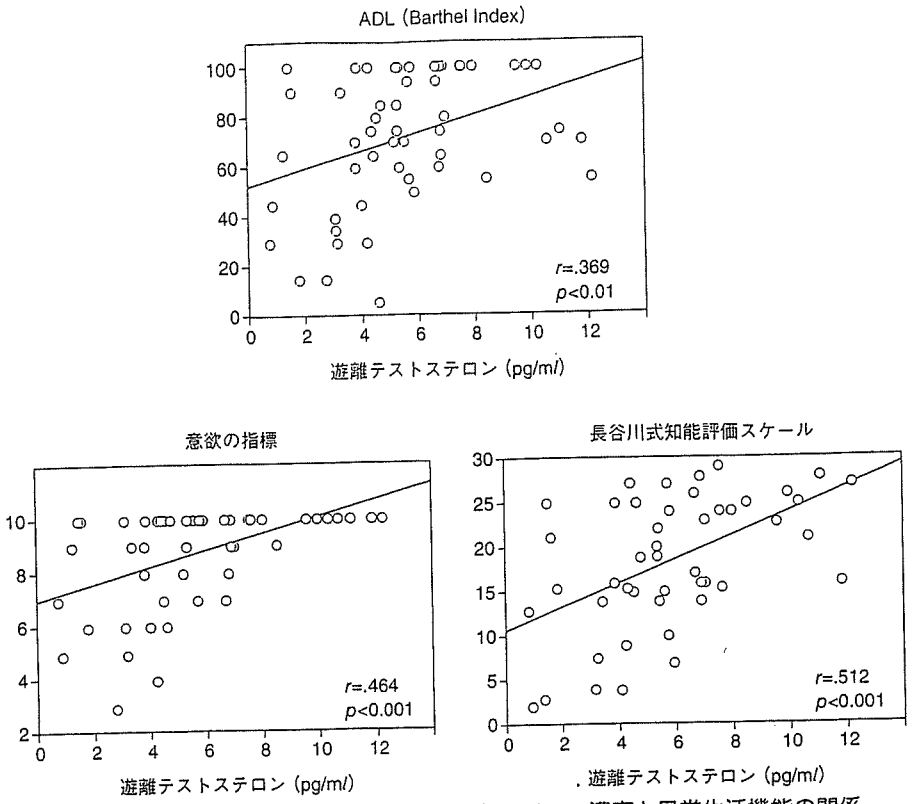

図 3　虚弱高齢男性における血中遊離テストステロン濃度と日常生活機能の関係
(Akishita M, et al. Testosterone and comprehensive geriatric assessment in frail elderly men. J Am Geriatr Soc 2003；51：1324-1326 より引用)

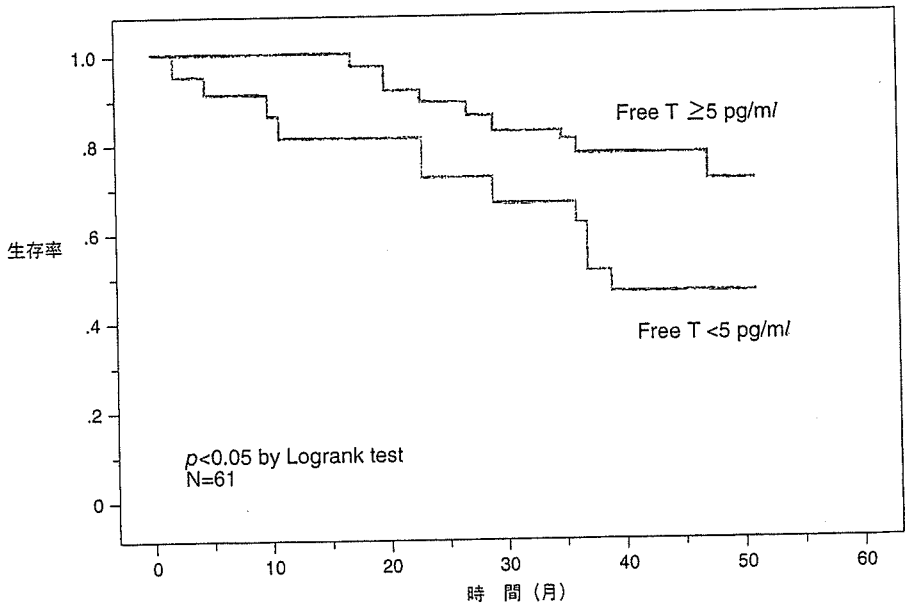

図 4　虚弱高齢男性の遊離テストステロン(Free-T)濃度と生命予後
介護を要する男性(平均 82 歳)の血清 Free-T 濃度を測定し，平均 3.1 年間追跡した

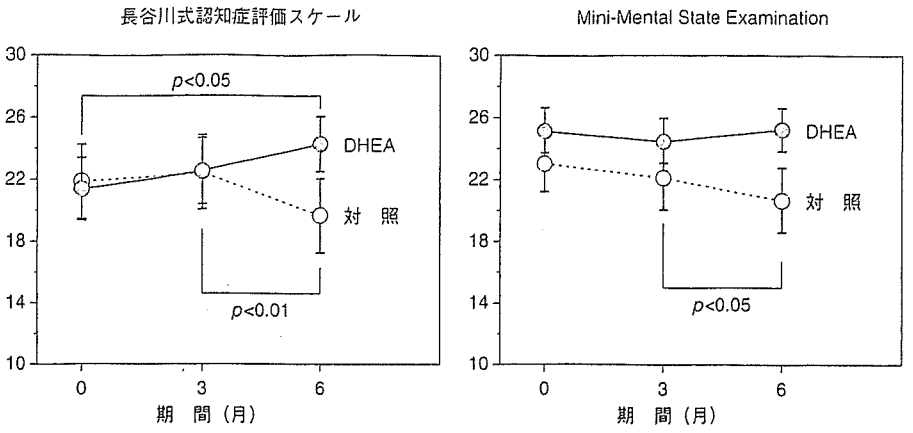

図 5 軽度認知機能障害を有する高齢女性に対する DHEA 補充療法の効果
軽度認知機能障害と診断された女性（平均 81 歳）に DHEA 25 mg/ 日を投与し，非投与群と比較した

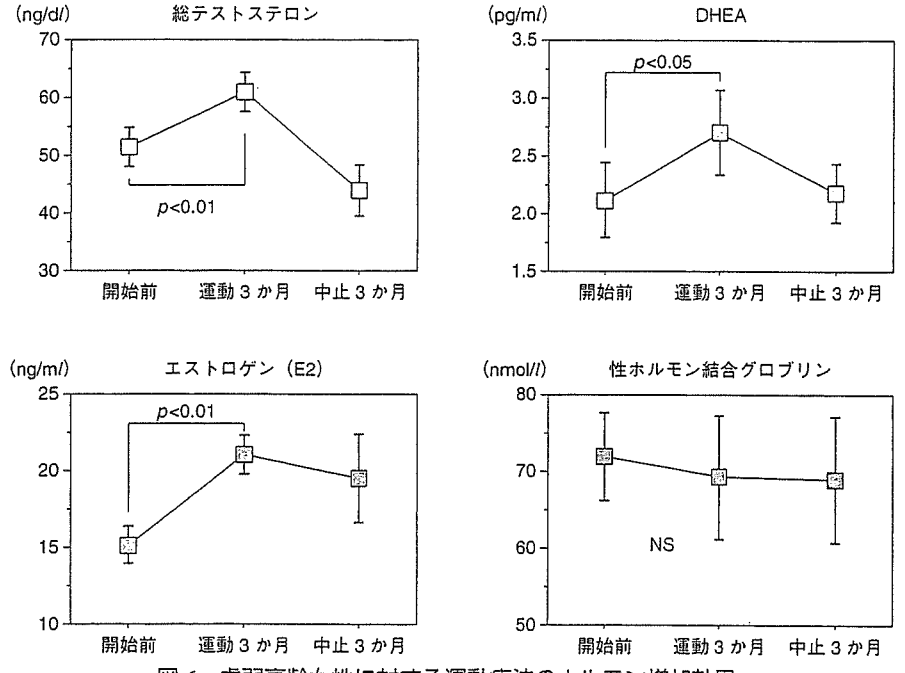

図 6 虚弱高齢女性に対する運動療法のホルモン増加効果
（Akishita M, et al. Effects of physical exercise on plasma concentrations of sex hormones in elderly women with dementia J Am Geriatr Soc. 2005；53：1076-1077 より引用）
グループホーム入所中の女性 13 名（平均 84 歳）に対し，イスおよびダンベルを用いた上下肢筋力トレーニングを連日 30 分間，3 か月間実施した

変化に加え，インスリン抵抗性，内臓脂肪蓄積が指摘されており，動脈硬化の進行に関わると考えられる．上述した Massachusetts Male Aging Study では，テストステロン低値がその後の 2 型糖尿病発症につながることを報告している．

アンドロゲン補充療法の動脈硬化とその危険因子に対する効果については，体脂肪の減少，インスリン感受性の改善，LDL コレステロールの低下といった代

謝性変化，心筋梗塞や脳卒中の引き金となる凝固系と炎症への作用が報告されているが，効果が認められなかったとする報告も同程度みられる．動脈硬化の進展，心筋梗塞や脳卒中など心血管イベントといった長期予後に対する効果は不明である．

アンドロゲンは高齢男性の生活機能にも影響している．介護を受けている男性では，総テストステロン濃度および遊離テストステロン濃度は，基本的 ADL，手段的 ADL，認知機能，意欲の指標と正相関した．特に遊離テストステロンと認知機能，意欲との関係は強く，年齢や各種栄養の指標で補正しても有意であった（図3）．一方，DHEA-S 濃度は認知機能とのみ相関した．興味あることに，この集団で遊離テストステロン濃度 5 pg/m*l* 未満の男性は，5 pg/m*l* 以上の男性に比べてその後 3 年間の死亡率が高かった（図4）．

2 女性におけるアンドロゲン低下と疾患

閉経後女性を 16 年間追跡した研究[3]では，骨粗鬆症の圧迫骨折に由来する身長低下に，開始時のテストステロン濃度は関連したがエストラジオールやエストロンは関連しなかった．同様に，DHEA-S 濃度が骨量と関連したことが複数報告されている．

多嚢胞性卵巣症候群の女性では高アンドロゲン血症と内臓肥満を呈するのに対し，閉経後女性ではアンドロゲン低値と関連して体脂肪（皮下脂肪＋内臓脂肪）蓄積を示す．テストステロン補充により内臓脂肪が減少したという報告もある．また，アンドロゲン低値は，男性と同様，閉経後女性における動脈硬化の進行にも関係しているようである．101 名の更年期女性（平均 47 歳）を対象に超音波で頸動脈肥厚を調べたイタリアの研究[4]では，DHEA-S 濃度が肥厚度と逆相

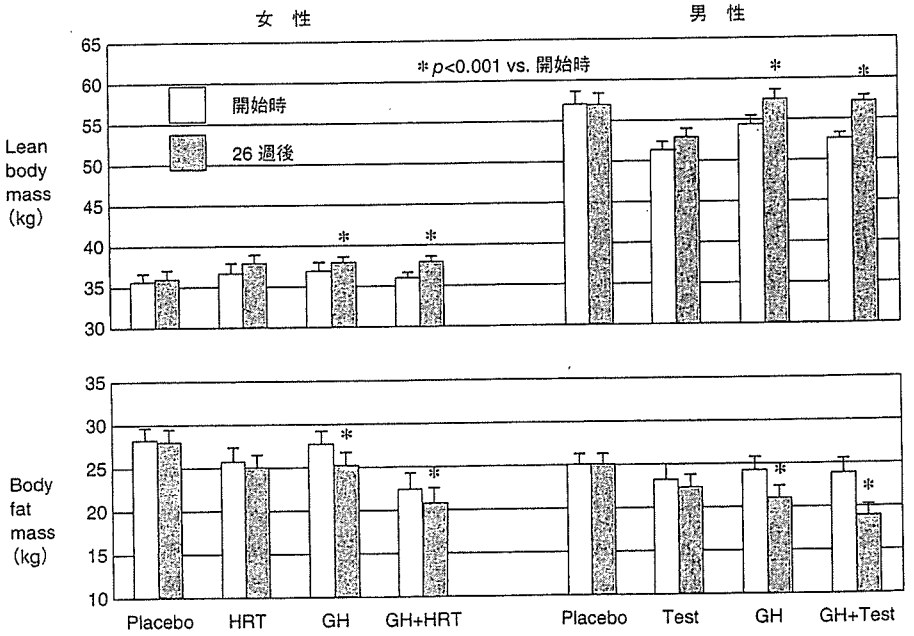

図7 高齢者における GH 補充療法の筋肉量および体脂肪量に対する効果
（Blackman MR, et al. Growth hormone and sex steroid administration in healthy aged women and men：a randomized controlled trial. JAMA 2002；288：2282-2292 より引用）
平均 72 歳の健常男女に対し，プラセボもしくは GH 投与（20 μg/kg 皮下注射，週3回）と，女性には HRT（エストロゲン＋プロゲスチン），男性にはテストステロン（Test）を組み合わせて投与した．筋肉量は lean body mass，体脂肪量は body fat mass として DXA 法で測定した

関した．

高齢女性でもDHEA-S濃度は生活機能と正相関する．また，軽度認知機能障害を有する高齢女性に対してDHEA補充療法を行ったところ，認知機能は有意に改善した（図5）．運動療法は高齢者の生活機能を改善し，転倒や心血管病のリスクを減らす効果があるとされる．認知症のグループホーム入所高齢女性（図6）に運動療法を行ったところ各種ホルモンの血中濃度が増加した．在宅高齢者の転倒予防運動教室でも同様の効果を確認しており，運動療法にはホルモン補充療法の代替療法としての意義も期待できる．

GHとIGF-1

GH欠乏は小児期には成長障害（小人症）をもたらし，成人でも筋肉減少と関係するが，加齢によるGH/IGF-1低下が老化とどの程度関係しているのか明らかでない．GH/IGF-1の濃度低下が骨量減少や体脂肪蓄積と関連したという報告があるが，その関係はアンドロゲンに比べると弱い印象がある．

GH補充療法の効果も，GH欠乏症に対しては明瞭であり，成人では自覚的健康感の改善，筋肉増加，体脂肪減少，各種代謝異常の改善が示されている．一方，明らかなGH欠乏症ではない高齢者にGHを投与した場合の効果も検討されている．女性ではHRTと組み合わせて，男性ではテストステロンと組み合わせてGH投与を行った無作為比較試験では，GHによりIGF-1濃度は2倍程度に上昇し，26週後には性ホルモンの有無にかかわらず筋肉量は増加し，体脂肪は減少した（図7）．同じグループの研究では，GH投与によりタンパク合成指標の増加，内臓脂肪の減少はみられたものの，骨量の有意な増加はみられなかった．また，耐糖能異常の発生がGH投与群で多くみられ，有害作用にも注意が必要である．

文　献

1) 岩本晃明ほか．日本人成人男子の総テストステロン，遊離テストステロンの基準値の設定．日泌尿会誌 2004；95：751-760.
2) Snyder PJ, Peachey H, Hannoush P, et al：Effect of testosterone treatment on bone mineral density in men over 65 years of age. J Clin Endocrinol Metab 1999；84：1966-1972.
3) Jassal SK, Barrett-Connor E, Edelstein SL：Low bioavailable testosterone levels predict future height loss in postmenopausal women. J Bone Miner Res 1995；10：650-654.
4) Bernini GP, Sgro' M, Moretti A, Argenio GF, Barlascini CO, Cristofani R, Salvetti A：Endogenous androgens and carotid intimal-medial thickness in women. J Clin Endocrinol Metab 1999；84：2008-2012.

Available online at www.sciencedirect.com
ScienceDirect
Biochemical and Biophysical Research Communications 353 (2007) 764–769
BBRC
www.elsevier.com/locate/ybbrc

Signaling pathway of nitric oxide production induced by ginsenoside Rb1 in human aortic endothelial cells: A possible involvement of androgen receptor

Jing Yu [a], Masato Eto [b], Masahiro Akishita [b], Akiyo Kaneko [a], Yasuyoshi Ouchi [b], Tetsuro Okabe [a,*]

[a] *Department of Integrated Traditional Medicine, University of Tokyo Graduate School of Medicine, Tokyo, Japan*
[b] *Department of Gerontology, University of Tokyo Graduate School of Medicine, Tokyo, Japan*

Received 7 December 2006
Available online 22 December 2006

Abstract

Ginsenosides have been shown to stimulate nitric oxide (NO) production in aortic endothelial cells. However, the signaling pathways involved have not been well studied in human aortic endothelial cells. The present study was designed to examine whether purified ginsenoside Rb1, a major active component of ginseng could actually induce NO production and to clarify the signaling pathway in human aortic endothelial cells. NO production was rapidly increased by Rb1. The rapid increase in NO production was abrogated by treatment with nitric oxide synthetase inhibitor, L-NAME. Rb1 stimulated rapid phosphorylation of Akt (Ser473), ERK1/2 (Thr202/Thr204) and eNOS (Ser1177). Rapid phosphorylation of eNOS (Ser1177) was prevented by SH-5, an Akt inhibitor or wortmannin, PI3-kinase inhibitor and partially attenuated by PD98059, an upstream inhibitor for ERK1/2. Interestingly, NO production and eNOS phosphorylation at Ser1177 by Rb1 were abolished by androgen receptor antagonist, nilutamide. The results suggest that PI3kinase/Akt and MEK/ERK pathways and androgen receptor are involved in the regulation of acute eNOS activation by Rb1 in human aortic endothelial cells.

Keywords: Ginsenoside Rb1; Endothelial cells; Nitric oxide; eNOS; Androgen receptor; P13-kinase; Akt; ERK; MEK; Phosphorylation

Ginseng, the root of Panax ginseng C.A. Meyer (Araliaceae), is a well-known and popular herbal medicine used worldwide. Among more than 30 ginsenosides, the active ingredient of ginseng, ginsenoside Rb1 is regarded as the main compound responsible for many pharmaceutical actions of ginseng. The oral administration of ginseng caused a decrease in blood pressure in essential hypertension [1]. Intravenous administration of ginsenosides (a mixture of saponin from Panax ginseng C.A. Meyer) lowered blood pressure in a dose-dependent manner in anesthetized rats [2]. Although these reports suggest that ginsenosides could stimulate the production of nitric oxide (NO) by aortic vascular endothelial cells, the precise mechanisms of the ginsenoside actions have not been fully elucidated [3]. NO released from endothelial cells via the endothelial nitric oxide synthetase (eNOS) is a pivotal vasoprotective molecule. In addition to its vasodilating feature, endothelial NO has anti-atherosclerotic properties, such as inhibition of platelet aggregation, leukocyte adhesion, smooth muscle cell proliferation, and expression of genes involved in atherosclerosis [4].

The present study aims at investigating the signaling pathways involved in NO production by purified ginsenoside Rb1 in human aortic endothelial cells in vitro.

Materials and methods

Materials. Rb1, nilutamide, L-NAME (hydrochloride), Hanks' balanced salt solution (HBSS) were purchased from Sigma (St. Louis, MO,

* Corresponding author. Fax: +813 5684 3987.
E-mail address: okabe-tky@umin.ac.jp (T. Okabe).

0006-291X/$ - see front matter © 2006 Elsevier Inc. All rights reserved.
doi:10.1016/j.bbrc.2006.12.119

USA). ICI182780 was from Zeneca Pharmaceuticals (Macdesfield, UK). 4,5-diaminofluorescin diacetate (DAF-2 DA) was purchased from Daiichi (Daiichi Pure Chemicals Co., Ltd, Tokyo, Japan). PD98059, SH-5, wortmannin and Nitric Oxide Synthase Assay Kit were from Calbiochem (EDM Biosciences, Inc., La Jolla, CA, USA and Germany). L-[^{3}H]Arginine was purchased from Amersham (Amersham Biosciences, Uppsala, Sweden). Antibody of phospho-eNOS (Ser1177) was from upstate (Upstate Inc., Lake Placid, NY). Antibody for eNOS/NOS type III was purchased form BD Transduction Laboratories (BD Biosciences, Franklin Lakes, NJ, USA). All other antibodies were form Cell Signaling Technology (Beverly, MA, USA). LumiGLO Reserve Chemiluminescent Substrate Kit was from KPL (Gaithersburg, MD, USA). EBM-2 (endothelial cell base medium) was from Clonetics (Walkersville, MD, USA). Human aortic endothelial cells (HAECs) were from Cambrex (Cambrex BioScience Walkersville, Inc. Walkersville, MD, USA). Fetal bovine serum (FBS) was from CCT (Sanko Junyaku Co., Ltd, Tokyo, Japan), Fetal bovine serum charcoal stripped was from MultiSer (ThermoTrace Ltd., Melbourne, Australia).

Cell culture. HAECs were cultured in a 37 °C humidified atmosphere of 95% air/5% CO_2 in EGM-2 (endothelial cell grows medium 2) medium supplemented with 10% FBS. The EGM-2 medium consisted of 0.1% EGF, 0.04% hydrocortisone, 0.4% hFGF-B, 0.1% VEGF, 0.1% R^3-IGF-1, 0.1% ascorbic acid, 0.1% GA-1000, and 0.1% heparin. Experiments were performed with cells from passages 5 to 7. For all experiments, HAECs were plated at a concentration of 1×10^4/mL and grown to confluence. Then cells were serum-starved for 6 h in phenol red free EBM-2 containing 1% DCC-FBS, that was removed the steroid by processing it with dextran-coated charcoal (DCC-FBS). In some inhibitory experiments, the inhibitors were added to cells 60 min before the stimuli. DMSO was used as a solvent for Rb1, PD98059, wortmannin, SH-5, L-NAME, nilutamide, and DAF-2 DA present at equal concentrations (0.01%) in all groups, including the vehicle.

Western blot analysis. After treatment with reagents, confluent monolayers of cells were washed two times in ice-cold phosphate-buffered saline and lysed with buffer containing 20 mmol/L Tris–HCl (pH 7.5), 150 mmol/L NaCl, 1 mmol/L EDTA, 1 mmol/L EGTA, 1% Triton-X, 2.5 mmol/L sodium pyrophosphate, 1 mmol/L β-glycerophosphate, 1 mmol/LNa_3VO_4, 1 μg/mL Leupeptin, 1 mM PMSF). For western blot analysis, total cell lysate was subjected to SDS–polyacrylamide gel electrophoresis (PAGE), and proteins were transferred to poly vinilidene difluoride (PVDF) membrane. The antibodies used in this study were anti-phospho-ERK1/2 (Thr202/Thr204), anti-ERK1/2, anti phospho-Akt (Ser473), anti-Akt, anti-phosph-eNOS (ser1177) and anti-NOS. Antibodies were detected by means of a horseradish peroxidase-linked secondary antibody and immunoreactive bands were visualized using LumiGLO Reserve Chemiluminescent Substrate Kit.

Endothelial NO synthase activity assay. Endothelial cell NO synthase (eNOS) activity was quantified by measuring the conversion of L-[^{3}H]-arginine to L-[^{3}H]-citrulline by the use of a NO synthase assay kit.

Measurement of intracellular production of NO. Production of NO was assessed using the NO-sensitive fluorescent dye DAF-2 DA [5]. Briefly, confluent cells were serum-staved for 6 h. Because NOS generates O_2^- instead of NO in the absence of L-arginine, so L-arginine (100 μmol/L) was add 1 h prior to all solutions, except for the experiment with *N*-nitro-L-arginine methyl ester (L-NAME; a NOS inhibitor)-treated cells. Cells were loaded with DAF-2 DA (final concentration 5 μmol/L, 30 min 37 °C) and than rinsed three times with HBSS, kept in the dark, and maintained at 37 °C in 1% EBM-2 medium with a warming stage. After 30 min, cells were then treated with Rb1 or other stimuli. In some inhibitory experiments, the inhibitors were administered 30 min before loading with DAF-2 DA. Green fluorescence intensity was measured with a laser scanning confocal microscopy system (LSCM) (Bio-Rad Laser Sharp2000). The fluorescence image was obtained as a 512×512 pixel frame. Ex = 488 nm, EM = 510 nm. All other settings, including scanning speed, pinhole diameter, and voltage gain, remained the same for all experiments.

Statistics. Data are means ± SEM. Statistical comparisons were performed by Student's *T* test between two groups. A value of $P < 0.05$ was considered significant.

Results

Rb1 stimulates rapid production of NO in human aortic endothelia cells

We used the NO-specific fluorescent dye DAF-2 DA to evaluate the effect of Rb1 on NO production in HAECs. 5, 10, 15, 30, 60, 120 and 180 min after Rb1 treatment, cells were fixed and then viewed using a fluorescence microscope. Emission of green light (510 nm) from cells excited by light at 488 nm is indicative of NO production. A significant increase in green fluorescence was observed >15 min after the addition of Rb1 and lasted for 60 min in HAECs (Fig. 1A). Maximal stimulation of NO production was obtained at 30 min.

To verify that the rapid increase in green fluorescence in response to Rb1 treatment specifically reflected NO production, we compared results from HAECs treated with acetylcholine (1 μmol/L) or Rb1 (1 μmol/L) for 5 min. Reassuringly, treatment with either acetylcholine and calcium ionophore or Rb1 resulted in a increase in green fluorescence (Fig. 1B). We next examined the effects of the NOS inhibitor L-NAME to determine whether the NO increase was attributable to NOS derived de novo synthesis. As shown in Fig. 1C, the Rb1-induced DAF-2 DA fluorescence was completely suppressed by pretreatment with L-NAME (0.5 mmol/L). The results suggested that the rapid increase in NO production after Rb1 treatment was mediated by an increase in NOS activity.

Rb1 stimulates phosphorylation of eNOS (Ser1177) and increases NOS activity

To examine involvement of eNOS in the NO increase, the effect of Rb1 on eNOS phosphorylation at Ser-1177 was tested by Western blotting. As shown in Fig. 2, Rb1 induced rapid eNOS phosphorylation after 10 min of incubation, maximal eNOS phosphorylation by Rb1 was observed from 30 to 60 min of incubation. The relative magnitude of eNOS phosphorylation falls subsequently but is still significantly greater than control after 120 min of Rb1 incubation (Fig. 2A, upper blots). The acute effect by Rb1 on eNOS phosphorylation was concentration dependent (Fig. 2B, upper blots). Rb1 did not affect eNOS protein expression (Fig. 2A and B, lower blots).

To see whether Rb1 actually activates NOS in HAECs, we measured NOS activity after 30 min of treatment with Rb1. As shown in Fig. 2C, Rb1 significantly increased NOS activity in HAECs.

PI3-kinase/Akt and MEK/ERK pathways are involved in eNOS phosphorylation and NO production

Previous studies have demonstrated that PI3-kinase/Akt and MEK/ERK pathways are two important signaling cascades mediating eNOS activation by many stimuli in vascular endothelial cells [6,7]. Therefore, we examined

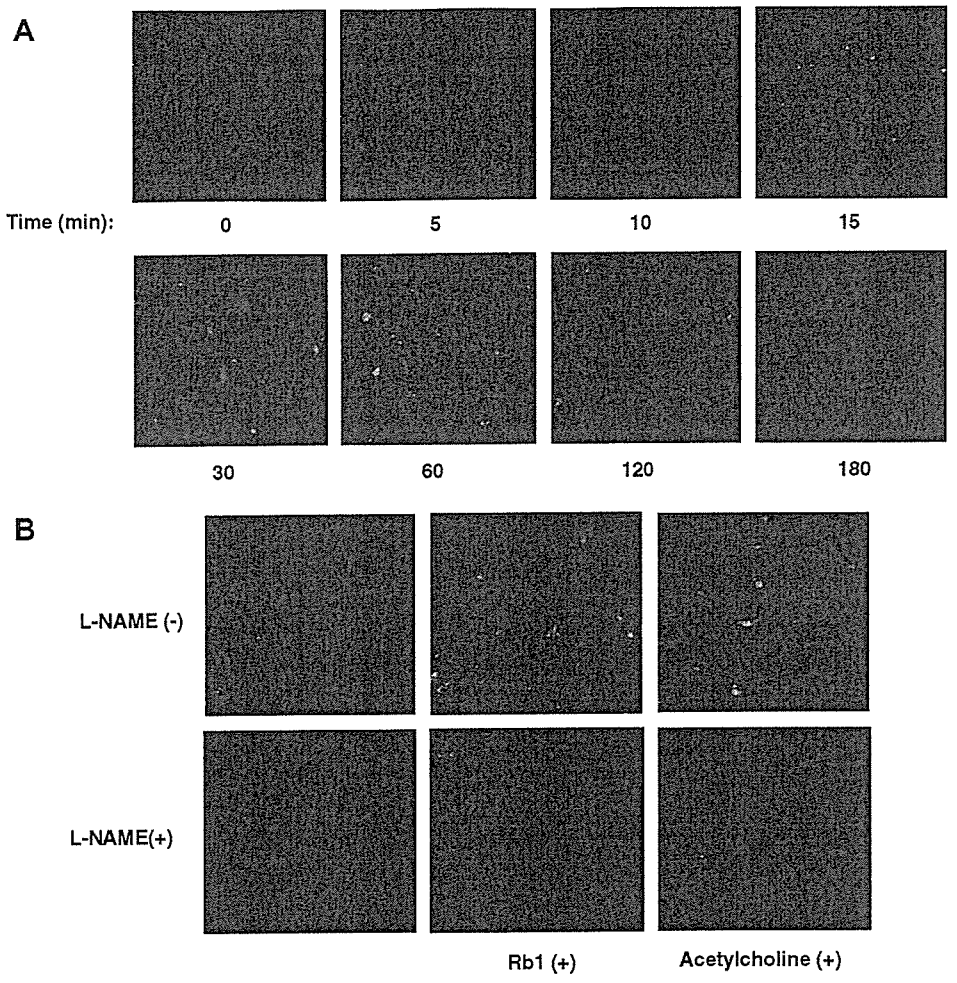

Fig. 1. Effect of Rb1 on production of NO. HAECs were starved and loaded with DAF-2 DA (5 μmol/L) as described in Materials and methods prior to treatment with either Rb1 (1 μmol/L) for 0, 5, 10, 15, 30, 60, 120, and 180 min (A) or acetylcholine (1 μmol/L) for 5 min (B). After Rb1 treatment, cells were fixed in 2% paraformaldehyde for 10 min at 4 °C and then viewed using a fluorescent microscope. Emission of green light (510 nm) from cells excited by light at 488 nm is indicative of NO production. In some groups of cells, L-NAME (0.5 mmol/L) was added 30 min before loading cells with DAF-2 DA (B). A representative time course experiment is shown for experiments that were repeated independently for three times. (For interpretation of the references to color in this figure legend, the reader is referred to the web version of this paper.)

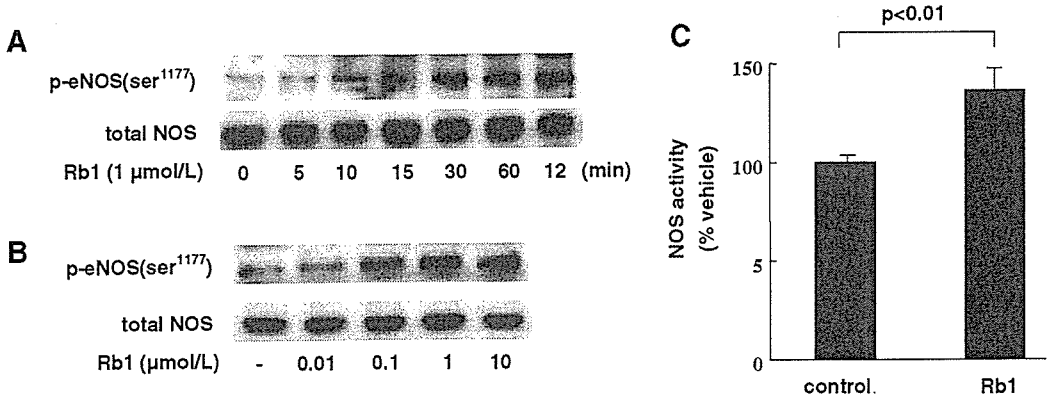

Fig. 2. Effects of Rb1 on eNOS phosphorylation and NOS activity. Phosphorylation of eNOS in HAECs. Starved HAECs were treated with the vehicle (0.01% DMSO) or Rb1 (1 μmol/L) for indicated times (A) or with various concentrations of Rb1 for 30 min (B). Western analysis performed to detect phospho-eNOS (Ser1177) and total eNOS. The experiments were repeated three times in triplicates, with equal result. NOS activity in HAECs homogenates. Rb1 (1 μmol/L) were added to the starved medium for 30 min, then activity of NOS was measured by the conversion of L-arginine to L-citrulline at 37 °C for 60 min (C). Histograms and error bars represent means ± SEM of four independent experiments performed in duplicate. $^{*}P < 0.01$ vs control.

whether Rb1 activated Akt and ERK1/2. We used phospho-specific antibodies to evaluate the ability of Rb1 to stimulate phosphorylation of Akt and ERK1/2 in HAECs. Rb1 rapidly increased phosphorylation of Akt (Ser473) and ERK1/2 (Fig. 3A, upper blots) in HAECs > 5 min after the addition of Rb1. Maximal phosphorylation was attained at 30 min in Akt and at 15 min in ERK1/2. The relative magnitude of the Rb1 response falls subsequently but is still significantly greater than control after 120 min of Rb1 treatment. Rb1 did not affect total Akt and ERK protein expression (Fig. 3A, lower blots).

We next examined the rapid phosphorylation of eNOS at Ser1179 by Rb1 either in the absence or presence of PI3 kinase inhibitor wortmannin, and Akt inhibitor SH-5 or MEK (ERK kinase) inhibitor PD98059. As shown in Fig. 3B, the rapid eNOS phosphorylation was abolished by pretreatment of cells with wortmannin (5 μmol/L) or SH-5, and partially attenuated by MEK inhibitor PD98059 (10 μmol/L). NO production viewed by fluorescent microscopy showed the similar inhibition by these inhibitors (Fig. 3C). These results suggest that acute activation of eNOS and NO production by Rb1 were mediated through activation of PI3-kinase/Akt and ERK1/2.

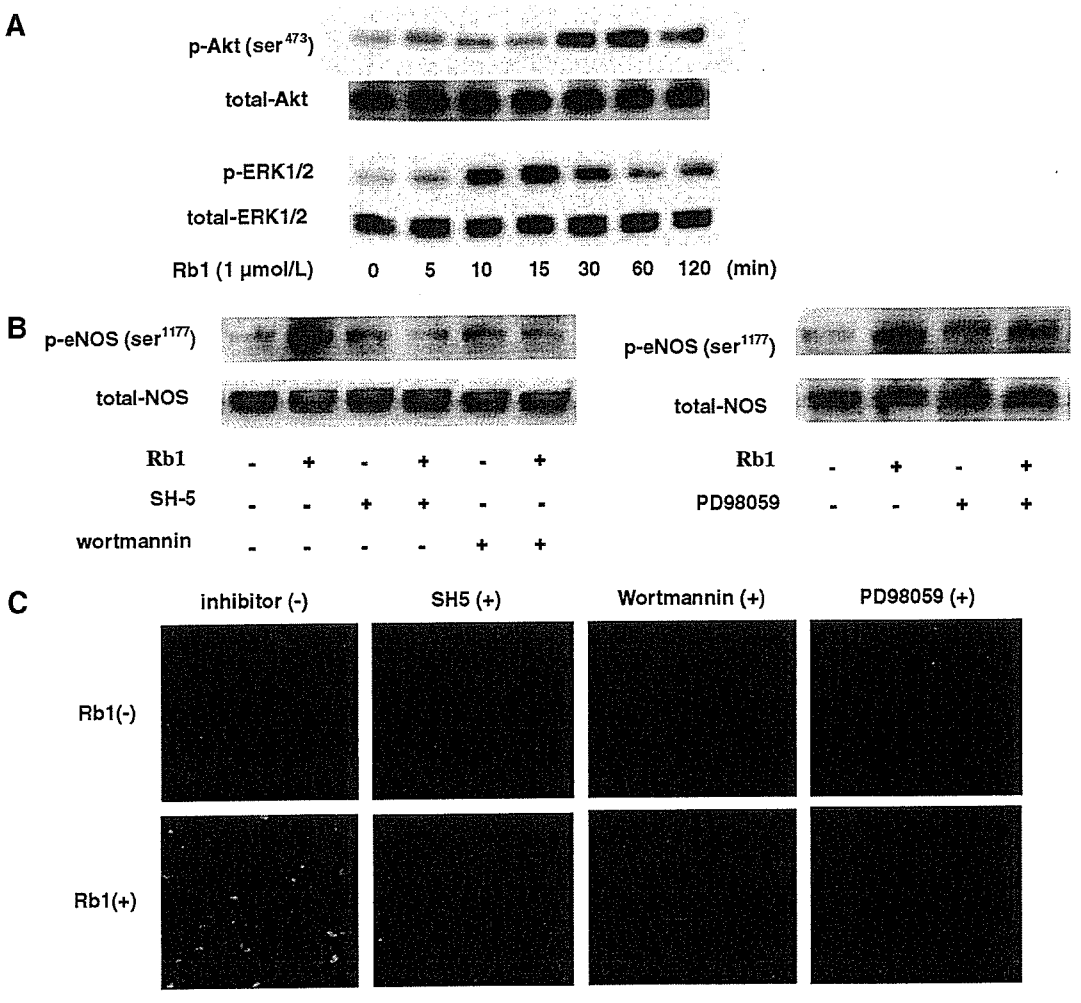

Fig. 3. Effects of inhibitors for PI3kinae/Akt or MEK (ERK kinase) on eNOS phosphorylation and NO production. Starved HAECs were treated with the vehicle (0.01% DMSO) or Rb1 (1 μmol/L) for indicated times (A). In some groups, cells were pretreated with SH-5 (10 μmol/L), wortmannin (5 μmol/L) or PD98059 (10 μmol/L) for 1 h, then cells were treated without or with Rb1 (1 μmol/L) for 30 min (B). Cell lysates were analyzed by Western blot as described in Materials and methods. Anti-phospho-Akt (Ser473) antibody and anti-Akt antibody; anti-phospho-ERK1/2 antibody and anti-ERK1/2 antibody (A), anti-phospho-eNOS (Ser1177) antibody and anti-eNOS antibody (B) were used for western blot analysis. Experiments were repeated three times, with equivalent result. Starved cells were loaded with DAF-2 DA as described in Materials and methods before treatment with Rb1 (1 μmol/L). In some groups of cells, SH-5 (10 μmol/L), wortmannin (5 μmol/L) or PD98059 (10 μmol/L) were added 60 min before cells were loaded with DAF-2 DA. After Rb1 treatment, cells were fixed in 2% paraformaldehyde for 10 min at 4 °C and then viewed using a fluorescent microscope (C). Emission of green light (510 nm) from cells excited by light at 488 nm is indicative of NO production. A representative set of experiments is shown for experiments that were repeated independently three times. (For interpretation of the references to color in this figure legend, the reader is referred to the web version of this paper.)

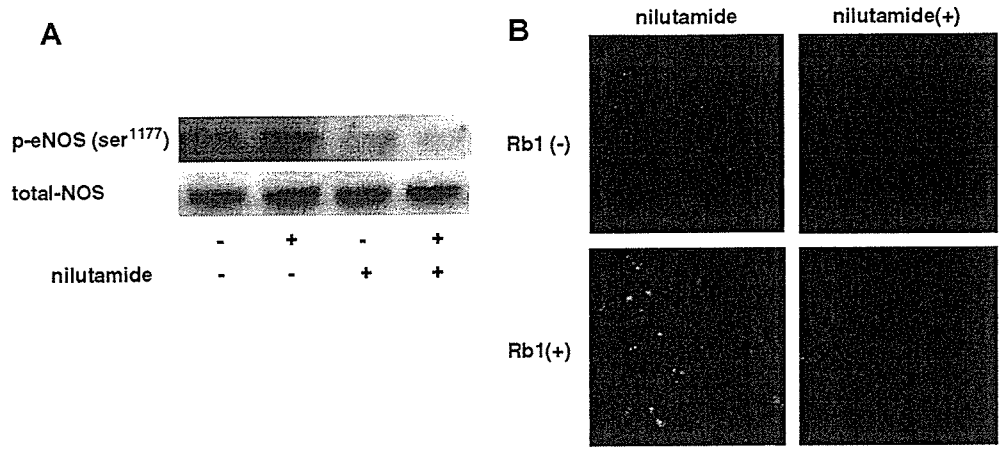

Fig. 4. Effects of nilutamide, an antagonist of androgen receptor, on eNOS phosphorylation and NO production. HAECs were starved 6 h and then treated without or with Rb1 (1 μmol/L) for 30 min. Some groups of cells were pre-treated with androgen receptor agonist nilutamide (10 μmol/L) for 1 h. Cell lysates were then subjected to immunoblotting as described in Materials and methods. The experiments were repeated three times in triplicates, with equal results. Starved cells were loaded with DAF-2 DA as described in Materials and methods before treatment with Rb1 (1 μmol/L). In some groups of cells, nilutamide (10 μmol/L) were added 60 min before cells were loaded with DAF-2 DA. After Rb1 treatment, cells were fixed in 2% paraformaldehyde for 10 min at 4 °C and then viewed using a fluorescent microscope (B). Emission of green light (510 nm) from cells excited by light at 488 nm is indicative of NO production. The experiments were repeated independently three times with equal results. (For interpretation of the references to color in this figure legend, the reader is referred to the web version of this paper.)

Rb1-induced eNOS phosphorylation is inhibited by androgen receptor antagonist

Increasing evidence shows that activation of the steroid hormone receptor such as estrogen receptor (ER) lead to NO production and vasodilation within minutes by non-transcriptional pathways. Ginsenosides have steroidal skeleton structure and can act as an agonist for steroid hormones receptor. To see whether steroid hormone receptors were involved in acute activation of eNOS to produce NO in HUACs by Rb1, we examined the effects of the androgen receptor antagonist nilutamide and estrogen receptor antagonist ICI182780. Representative western blots obtained using anti-phospho-eNOS (Ser1177) antibody and anti-eNOS antibody are shown in Fig. 4A. The Rb1-induced eNOS phosphorylation (Ser1177) was inhibited by the androgen receptor antagonist nilutamid (10 μmol/L) In addition, NO production was diminished to the baseline level in the presence of nilutamid (Fig. 4B). However, the Rb1-induced eNOS phosphorylation (Ser1177) and NO production were unaffected by an estrogen receptor (ER) antagonist ICI182780 (10 μmol/L) (data not shown).

Discussion

We have shown that purified Rb1 rapidly stimulates production of NO in HAECs > 15 min after treatment. Maximal stimulation of NO production was obtained at 30 min. The increase in NO production was abrogated by the addition of eNOS inhibitor, L-NAME. It is generally well known that eNOS is tightly regulated not only at the transcriptional level but also by several post-transcriptional mechanisms [8]. The enhanced phosphorylation at Ser1177 leads to increased eNOS activity. In our experiments, Rb1 induced rapid phosphorylation of eNOS at Ser1177 > 10 min after Rb1 treatment. Maximal eNOS phosphorylation by Rb1 was observed from 30 to 60 min of incubation. NOS activity was also increased by the addition of Rb1 in HAECs. Taken together, our results suggest that the acute effect on NO production in HAECs is attributable to rapid phosphorylation of eNOS at Ser1177. NO produced by eNOS is a fundamental determinant of cardiovascular homeostasis responsible for regulating systolic blood pressure, vascular remodeling and angiogenesis. It is possible to consider that Rb1, a major active component of ginseng could be a candidate responsible for the antihypertensive effects of ginseng previously reported [1,2].

Recent studies have revealed that PI3-kinase/Akt and MEK/ERK1/2 pathways are crucial regulator in cell proliferation, cell-cycle progression, and mediator of cellular survival. Both of them also contribute to enhanced phosphorylation of eNOS at Ser1177/1179 and production of NO [6,7]. The present study showed that Rb1 also stimulated the phosphorylation of Akt (Ser473) and ERK1/2 (Thr202/Thr204) in HAECs. Rb1-induced eNOS phosphorylation was prevented by inhibitors for PI3-kinase/Akt or MEK (ERK kinase). Our data suggest that the activation of PI3-kinase/Akt and MEK/ERK-mediated pathways are involved in the regulation of acute eNOS phosphorylation by ginsenoside Rb1 in HAECs.

Another interesting finding is that acute phosphorylation of eNOS by Rb1 was abolished by an antagonist for androgen receptor. Recent studies have shown Rb1 acts as a phytoestrogen in MCF-7 human mammary carcinoma

cells [9]. However, in HAECs, Rb1-induced eNOS phosphorylation was not prevented by an antagonist for estrogen receptor (data not shown). It is known that testosterone prevents coronary artery disease, and lower testosterone level is a risk factor for ischemic heart disease in men [10–12]. Recent studies revealed that endothelial NO has antiatherosclerotic properties, such as inhibition of platelet aggregation, leukocyte adhesion, smooth muscle cell proliferation, and expression of genes involved in atherosclerosis [4]. Together with these observations, our results that Rb1 induced eNOS phosphorylation has been abolished by the androgen receptor antagonist will be the beginning of the experimental analyses at cellular levels and may provide a clue for better understanding of the mechanisms by which androgens exert their action for preventing coronary artery disease. Further studies are required for elucidation.

Acknowledgments

We thank Drs. K. Yamamoto, K. Hasegawa, Y. Iwaoka, and S. Takasugi for their helpful advices and continuous encouragement.

References

[1] K.H. Han, S.C. Choe, H.S. Kim, D.W. Sohn, K.Y. Nam, B.H. Oh, M.M. Lee, Y.B. Park, Y.S. Choi, J.D. Seo, Y.W. Lee, Effect of red ginseng on blood pressure in patients with essential hypertension and white coat hypertension, Am. J. Chin. Med. 26 (1998) 199–209.

[2] N.D. Kim, S.Y. Kang, V.B. Schini, Ginsenosides evoke endothelium-dependant vascular relaxation in rat aorta, Gen. Pharmacol. 25 (1994) 1071–1077.

[3] N.D. Kim, S.Y. Kang, J.H. Park, V.B. Schini-Kerth, Ginsenoside Rg3 mediates endothelium-dependent relaxation in response to ginsenosides in rat aorta: role of K^+ channels, Eur. J. Pharmacol. 367 (1999) 41–49.

[4] A.G. Herman, S. Moncada, Therapeutic potential of nitric oxide donors in the prevention and treatment of atherosclerosis, Eur. Heart J. 26 (2005) 1945–1955.

[5] H. Kojima, N. Nakatsubo, K. Kikuchi, S. Kawahara, Y. Kirino, H. Nagoshi, Y. Hirata, T. Nagano, Detection and imaging of nitric oxide with novel fluorescent indicators: diaminofluoresceins, Anal. Chem. 70 (1998) 2446–2453.

[6] X. Peng, S. Haldar, S. Deshpande, K. Irani, D.A. Kass, Wall stiffness suppresses Akt/eNOS and cytoprotection in pulse-perfused endothelium, Hypertension 41 (2003) 378–381.

[7] D. Feliers, X. Chen, N. Akis, G.G. Choudhury, M. Madaio, B.S. Kasinath, VEGF regulation of endothelial nitric oxide synthase in glomerular endothelial cells, Kidney Int. 68 (2005) 1648–1659.

[8] I. Fleming, R. Busse, Molecular mechanisms involved in the regulation of the endothelial nitric oxide synthase, Am. J. Physiol. Regul. Integr. Comp. Physiol. 284 (2003) R1–R12.

[9] J. Cho, W. Park, S. Lee, W. Ahn, Y. Lee, Ginsenoside-Rb1 from Panax ginseng C.A. Meyer activates estrogen receptor-alpha and -beta, independent of ligand binding, J. Clin. Endocrinol. Metab. 89 (2004) 3510–3515.

[10] G.B. Phillips, B.H. Pinkernell, T.Y. Jing, The association of hypotesteronemia with coronary artery disease in men, Arterioscler. Thromb. 14 (1994) 701–706.

[11] C.M. Webb, J.G. McNeill, C.S. Hayward, D. De Zeigler, P. Collins, Effects of testosterone on coronary vasomotor regulation in men with coronary heart disease, Circulation 100 (1999) 1690–1696.

[12] F.C. Wu, A. von Eckardstein, Androgens and coronary artery disease, Endocr. Rev. 24 (2003) 183–217.

Available online at www.sciencedirect.com
ScienceDirect
European Journal of Pharmacology 556 (2007) 1–8
ejp
www.elsevier.com/locate/ejphar

Gas6/Axl-PI3K/Akt pathway plays a central role in the effect of statins on inorganic phosphate-induced calcification of vascular smooth muscle cells

Bo-Kyung Son [a], Koichi Kozaki [b], Katsuya Iijima [a], Masato Eto [a], Toru Nakano [c], Masahiro Akishita [a], Yasuyoshi Ouchi [a,*]

[a] *Department of Geriatric Medicine, Graduate School of Medicine, The University of Tokyo, 7-3-1 Hongo, Bunkyo-ku, Tokyo 113-8655, Japan*
[b] *Department of Geriatric Medicine, Kyorin University School of Medicine, Tokyo, Japan*
[c] *Discovery Research Laboratory, Shionogi and Co., Ltd., Osaka, Japan*

Received 19 May 2006; received in revised form 22 September 2006; accepted 27 September 2006
Available online 18 October 2006

Abstract

Apoptosis is essential for the initiation and progression of vascular calcification. Recently, we showed that *3-hydroxy-3-methylglutaryl* (HMG) CoA reductase inhibitors (statins) have a protective effect against vascular smooth muscle cell calcification by inhibiting apoptosis, where growth arrest-specific gene 6 (Gas6) plays a pivotal role. In the present study, we clarified the downstream targets of Gas6-mediated survival signaling in inorganic phosphate (Pi)-induced apoptosis and examined the effect of statins. We found that fluvastatin and pravastatin significantly inhibited Pi-induced apoptosis and calcification in a concentration-dependent manner in human aortic smooth muscle cells (HASMC), as was found with atorvastatin previously. Gas6 and its receptor, Axl, expression were downregulated in the presence of Pi, and recombinant human Gas6 (rhGas6) significantly inhibited apoptosis and calcification in a concentration-dependent manner. During apoptosis, Pi suppressed Akt phosphorylation, which was reversed by rhGas6. Wortmannin, a specific *phosphatidylinositol 3-OH kinase* (PI3K) inhibitor, abolished the increase in Akt phosphorylation by rhGas6 and eliminated the inhibitory effect of rhGas6 on both Pi-induced apoptosis and calcification, suggesting that PI3K-Akt is a downstream signal of the Gas6-mediated survival pathway. Pi reduced phosphorylation of Bcl2 and Bad, and activated caspase 3, all of which were reversed by rhGas6. The inhibitory effect of statins on Pi-induced apoptosis was accompanied by restoration of the Gas6-mediated survival signal pathway: upregulation of Gas6 and Axl expression, increased phosphorylation of Akt and Bcl2, and inhibition of Bad and caspase 3 activation. These findings indicate that the Gas6-mediated survival pathway is the target of statins' effect to prevent vascular calcification.

Keywords: Calcification; Apoptosis; Gas6; Axl; Akt; Bcl2

1. Introduction

Vascular calcification, such as coronary and aortic calcification, is clinically important in the development of cardiovascular disease (Eggen, 1968). Two distinct forms of vascular calcification are well recognized. One is medial calcification, which occurs between the cell layers of smooth muscle cells and is related to aging, diabetes and chronic renal failure (Neubauer, 1971; Goodman et al., 2000). The other is atherosclerotic calcification, which occurs in the intima during the development of atheromatous disease (Wexler et al., 1996). In diabetic patients, medial calcification has been shown to be a strong independent predictor of cardiovascular mortality (Everhart et al., 1988).

We recently demonstrated that atorvastatin prevented inorganic phosphate (Pi)-induced calcification by inhibiting apoptosis, one of the important processes regulating calcification. This was mediated by growth arrest-specific gene 6 (Gas6), a vitamin K-dependent protein (Son et al., 2006). Gas6 binds to Axl, the predominant receptor for Gas6, on the cell surface and transduces the signal by Axl autophosphorylation (Mark et al., 1996). Gas6-Axl interaction has been shown to be implicated in the regulation of multiple cellular functions (Yanagita et al., 2001; Goruppi et al., 1996; Nakano et al., 1997; Fridell et al., 1998). Especially, they are known to protect a range of cell types

* Corresponding author. Tel.: +81 3 5800 8652; fax: +81 3 5800 6530.
E-mail address: youchi-tky@umin.ac.jp (Y. Ouchi).

0014-2999/$ - see front matter © 2006 Elsevier B.V. All rights reserved.
doi:10.1016/j.ejphar.2006.09.070

from apoptotic death (Goruppi et al., 1996, 1999; Healy et al., 2001). However, the downstream targets of Gas6-mediated signaling in Pi-induced apoptosis and the effect of statins on this pathway are poorly understood.

With respect to the targets of Gas6-Axl interaction, Lee et al. (2002) showed that activation of Akt is necessary for Gas6-dependent cell survival. Akt is an important mediator of metabolic and survival responses after growth factor stimulation. Akt is activated by phosphorylation, which is performed by phosphatidylinositol 3-OH kinase (PI3K), a kinase that is activated by Gas6-Axl interaction (Lee et al., 2002; Ming Cao et al., 2001). Activation of Akt leads to downstream signaling events including those associated with mitochondrial regulators of apoptosis such as Bcl2 and Bad.

In the present study, we examined the effect of statins using two different types: lipophilic fluvastatin and hydrophilic pravastatin. We investigated the effect of statins on Pi-induced apoptosis and calcification as well as on signaling components in this process. Consequently, we found that both statins restored the Gas6-mediated survival pathway, with upregulation of the expression of Gas6 and Axl, increased phosphorylation of Akt, Bcl2 and Bad; and finally inhibition of caspase 3 activation, resulting in the prevention of apoptosis and subsequent calcification in human aortic smooth muscle cells (HASMC).

2. Materials and methods

2.1. Materials

Pravastatin and fluvastatin were supplied by Sankyo Co. Ltd. and Tanabe Seiyaku Co., Ltd., respectively. Recombinant human Gas6 (rhGas6) was prepared as described previously (Ming et al., 2001). Wortmannin was purchased from Calbiochem. All other reagents were of analytical grade.

2.2. Cell culture

HASMC were obtained from Clonetics. They were cultured in Dulbecco's modified Eagle's medium (DMEM) supplemented with 20% *fetal bovine serum* (FBS), 100 U/ml penicillin and 100 mg/ml streptomycin at 37 °C in a humidified atmosphere with 5% CO_2. HASMC were used up to passage 8 for the experiments.

2.3. Induction and quantification of calcification

For Pi-induced calcification, Pi (a mixed solution of Na_2HPO_4 and NaH_2PO_4 whose pH was adjusted to 7.4) was added to serum-supplemented DMEM to a final concentration of 2.6 mM. After the indicated incubation period, cells were decalcified with 0.6 M HCl, and Ca content in the supernatant was determined by the *o*-cresolphthalein complexone method (C-Test, WAKO). The remaining cells were solubilized in 0.1 M NaOH/0.1% *sodium dodecyl sulfate* (SDS), and cell protein content was measured by Bio-Rad protein assay. Calcification was visualized by von Kossa's method. Briefly, the cells were fixed with 4% formaldehyde and exposed to 5% aqueous $AgNO_3$.

2.4. Induction and determination of apoptosis

Two different time courses were tested to investigate Pi-induced apoptosis and examine the effect of statins, under short-term (within 24 h) and long-term (up to 10 days) conditions (Son et al., 2006).

2.4.1. TdT-mediated dUTP nick end-labeling (TUNEL) assay

TUNEL assay to detect DNA fragmentation was performed using a commercially available kit (ApopTag Plus, Chemicon). Briefly, the samples were preincubated with equilibration buffer for 10 min, and subsequently incubated with terminal deoxyribonucleotidyl transferase in the presence of digoxigenin-conjugated dUTP for 1 h at 37 °C. The reaction was terminated by incubating the samples in stopping buffer for 30 min. After 3 rinses with *phosphate-buffered saline* (PBS), a fluorescein-labeled anti-digoxigenin antibody was applied for 30 min, and the samples were rinsed 4 times with PBS. The samples were then stained, mounted with DAPI (*4′,6-diamino-2-phenylindole*)/antifade, and examined by fluorescence microscopy.

2.4.2. Detection of DNA fragmentation by ELISA

Cytoplasmic histone-associated DNA fragments were determined with a cell-death detection ELISA^{plus} kit (Roche) as a quantitative index of apoptosis. Briefly, after the cells were incubated in lysis buffer for 30 min, 20 μl of the cell lysates was used for the assay. Following addition of substrate, colorimetric change was determined as the absorbance value measured at 405 nm.

2.5. Immunoblotting

The effect of Pi and statins on the expression of Gas6 and Axl, phosphorylation of Akt, Bcl2 and Bad, and activation of caspase 3 was examined at 12 h. The collected cell lysates were applied to SDS-polyacrylamide gels under reducing conditions, and transferred to a polyvinylidene difluoride (PVDF) membrane. Immunoblot analysis was performed using specific primary antibodies: anti-Axl, anti-Gas6 (Santa Cruz Biotechnology), anti-caspase 3, anti-Akt, anti-Bcl2, anti-phospho-Akt, anti-phospho-Bcl2, anti-phospho-Bad (Cell Signaling Technology), and anti-Bad (Transduction Laboratories). After incubation with horseradish peroxidase-conjugated secondary antibodies (Amersham Pharmacia), blots were visualized by enhanced chemiluminescence and autoradiography (ECL Plus, Amersham Pharmacia). Experiments were performed with at least three different cell populations.

2.6. Statistical analysis

All results are presented as mean±S.E.M. Statistical comparisons were made by ANOVA, unless otherwise stated. A value of $P<0.05$ was considered to be significant.

3. Results

3.1. Statins inhibit Pi-induced apoptosis and calcification in HASMC

In HASMC, a high Pi level (≥2.6 mM), comparable to that of hyperphosphatemia in end-stage renal disease, significantly induced calcification. Fluvastatin showed an inhibitory effect on Pi-induced calcification at as high a concentration as 0.1 μM (26.1±2.3% of control), while pravastatin showed the degree of effect at 50 μM (27.4±3.1% of control) (Fig. 1A). An inhibitory effect on Ca deposition was also found by von Kossa's staining (Fig. 1B). Both statins prevented Pi-induced apoptosis at the same concentrations as those at which they prevented calcification (Fig. 1C). An antiapoptotic effect of statins was also observed by TUNEL assay on day 6 (Fig. 1D).

3.2. Gas6 plays an important role in Pi-induced apoptosis

In the presence of 2.6 mM Pi, the expression of Gas6 and Axl was markedly downregulated (Fig. 2A). To investigate the role of Gas6 in Pi-induced apoptosis and calcification, first, we tested whether supplementation of rhGas6 could prevent Pi-induced apoptosis. In HASMC, rhGas6 significantly inhibited Pi-induced apoptosis in a concentration-dependent manner (Fig. 2B). Furthermore, during apoptosis, activated products of caspase 3 (17 and 19 kDa) were significantly increased by 2.6 mM Pi, which was reversed by rhGas6 (Fig. 2C). Next, we examined the effect of rhGas6 on calcification. Recombinant human Gas6 significantly inhibited Pi-induced calcification on day 6 in a concentration-dependent manner (Fig. 2D), suggesting that Gas6 plays an important role in Pi-induced apoptosis and calcification.

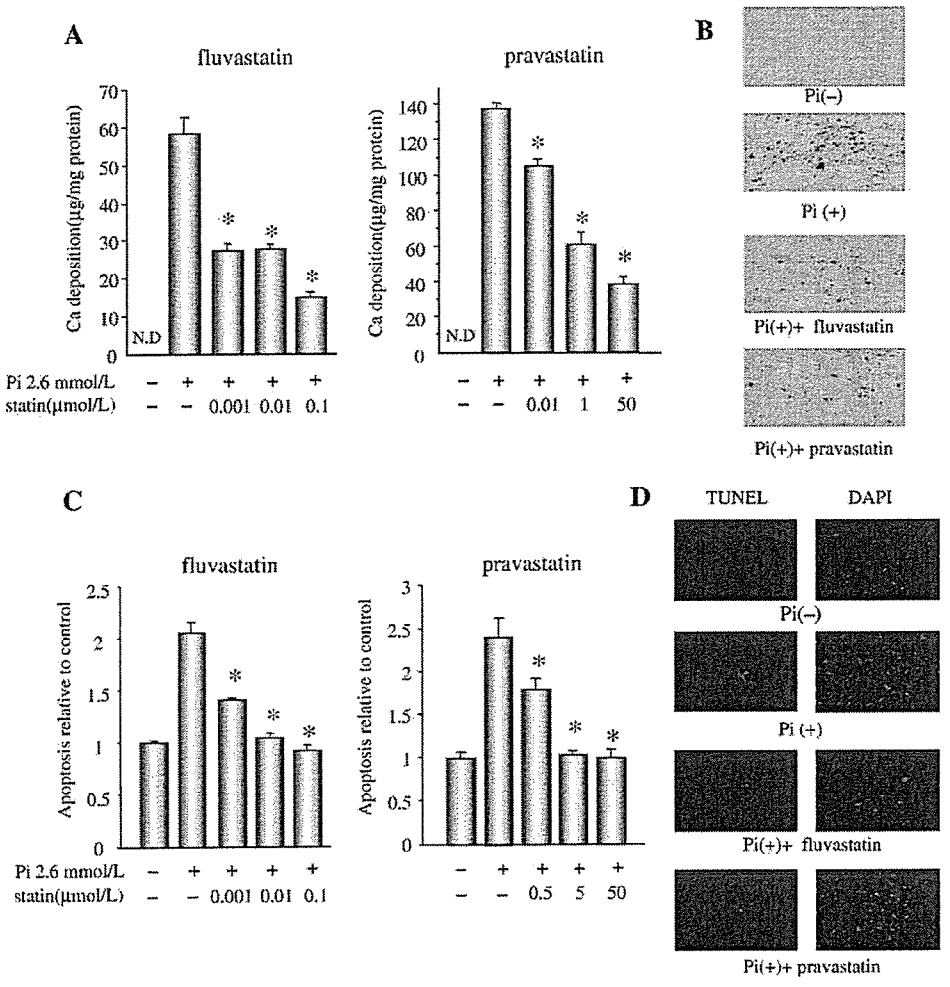

Fig. 1. Statins prevent Pi-induced apoptosis and calcification. HASMC were cultured with the indicated concentrations of fluvastatin and pravastatin in the presence of 2.6 mM Pi for 6 days. Ca deposition was measured by *o*-cresolphthalein complexone method, and normalized by cell protein content. All values are presented as mean± S.E.M. ($n=6$). *$P<0.05$ vs. statin (−) by Fisher's test. N.D. stands for "not detected" (A). On day 6, the inhibitory effect of fluvastatin (0.1 μM) and pravastatin (50 μM) on 2.6 mM Pi [Pi(+)]-induced Ca deposition was evaluated at the light microscopic level with von Kossa's staining (B). Serum-starved HASMC were cultured with the indicated concentrations of fluvastatin and pravastatin for 12 h and then incubated with 2.6 mM Pi for an additional 24 h. A quantitative index of apoptosis, determined by ELISA, is presented as the relative value to that without statins and 2.6 mM Pi. All values are presented as mean±S.E.M. ($n=3$). *$P<0.05$ vs. 2.6 mM Pi, statin (−) by Fisher's test (C). The antiapoptotic effect of fluvastatin (0.1 μM) and pravastatin (50 μM) was evaluated by TUNEL staining (green) on day 6. Nuclei were counterstained with DAPI (4′,6-diamino-2-phenylindole, blue) (D).

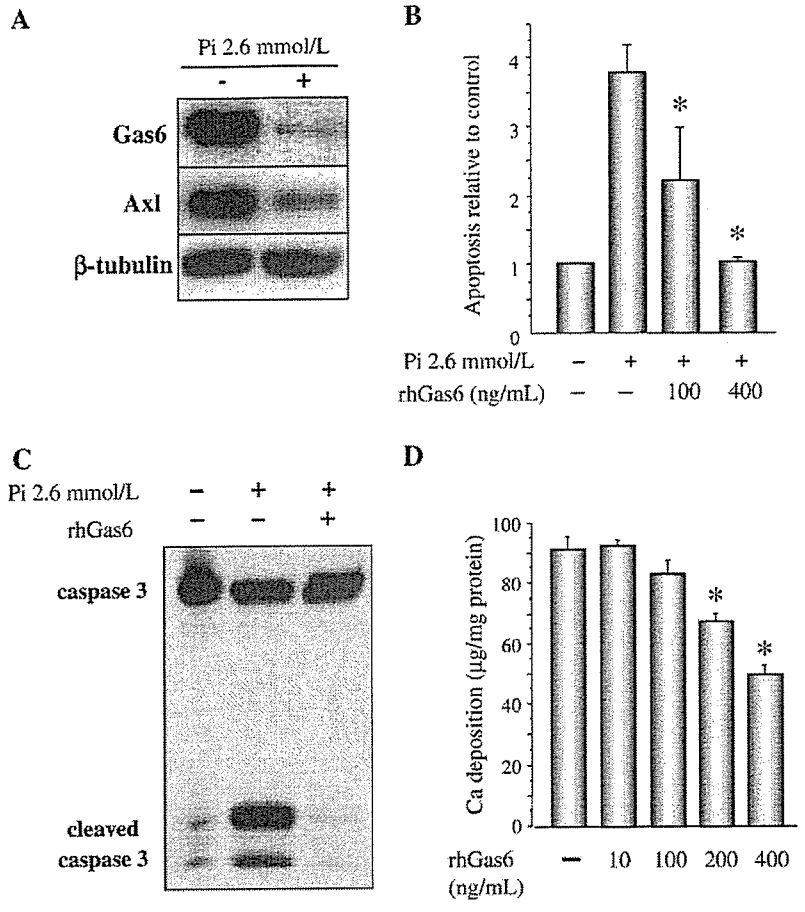

Fig. 2. Pi suppresses Gas6 and Axl expression, and rhGas6 inhibits caspase-dependent apoptosis and calcification. HASMC were cultured in the presence or absence of 2.6 mM Pi for 12 h. Cell lysates were collected and subjected to SDS-PAGE followed by immunoblotting with antibodies to Gas6, Axl or β-tubulin (A). After pretreatment with the indicated concentrations of rhGas6, apoptosis was induced by 2.6 mM Pi. All values are presented as mean±S.E.M. ($n=3$). *$P<0.05$ vs. 2.6 mM Pi, rhGas6 (−) by Fisher's test (B). HASMC were pretreated with rhGas6 (400 ng/ml) for 1 h, then cultured with 2.6 mM Pi for 12 h. Cell lysates were immunoblotted with an antibody that recognizes caspase-3 (35 kDa) and the cleaved forms of caspase-3 (17 and 19 kDa) (C). For measurement of Ca deposition, HASMC were cultured with the indicated concentrations of rhGas6 in the presence of 2.6 mM Pi for 6 days. All values are presented as mean±S.E.M. ($n=6$). *$P<0.05$ by Fisher's test (D). Experiments were performed with at least three different cell populations.

3.3. Downregulation of phospho-Akt participates in Pi-induced apoptosis

Since in NIH-3T3 fibroblasts, the antiapoptotic effect of Gas6-Axl interaction has been shown to be mediated by Akt phosphorylation (Goruppi et al., 1999), we examined whether Akt participates in the signaling of downregulation of the Gas6-Axl interaction during Pi-induced apoptosis. In the presence of 2.6 mM Pi, Akt phosphorylation was downregulated in a time-dependent manner, whereas the expression of total Akt was not changed (Fig. 3A). In addition, rhGas6 abrogated the Pi-induced decrease in Akt phosphorylation, implying that subsequent downregulation of Akt phosphorylation is the pathway of Pi-induced apoptosis (Fig. 3B).

Because Akt phosphorylation is regulated by PI3K, we examined the effect of wortmannin, a specific PI3K inhibitor, on rhGas6-mediated phosphorylation of Akt. As shown in Fig. 3B, wortmannin abrogated the rhGas6-induced phosphorylation of Akt and further eliminated the inhibitory effect of rhGas6 on Pi-induced apoptosis and calcification (Fig. 3C, D). These results indicate that the preventive effect of rhGas6 on Pi-induced apoptosis and calcification was mediated by the PI3K-Akt pathway.

3.4. Pi suppresses Bcl2 phosphorylation and activates Bad

To establish the downstream components of Pi-induced apoptosis, two key apoptosis-regulating proteins, Bcl2 and Bad, were analyzed. During apoptosis, phosphorylation of Bcl2 (active form) and Bad (inactive form) was markedly reduced by 2.6 mM Pi in a time-dependent manner. The expression level of their total protein was not changed in this period (Fig. 4A, B). By supplementation of the medium with rhGas6, the decrease in phosphorylation of Bcl2 and Bad by Pi was reversed to almost the basal level (Fig. 4C, D). These results indicate that Pi promotes apoptosis by inactivating Bcl2 and activating Bad via a Gas6-dependent pathway.

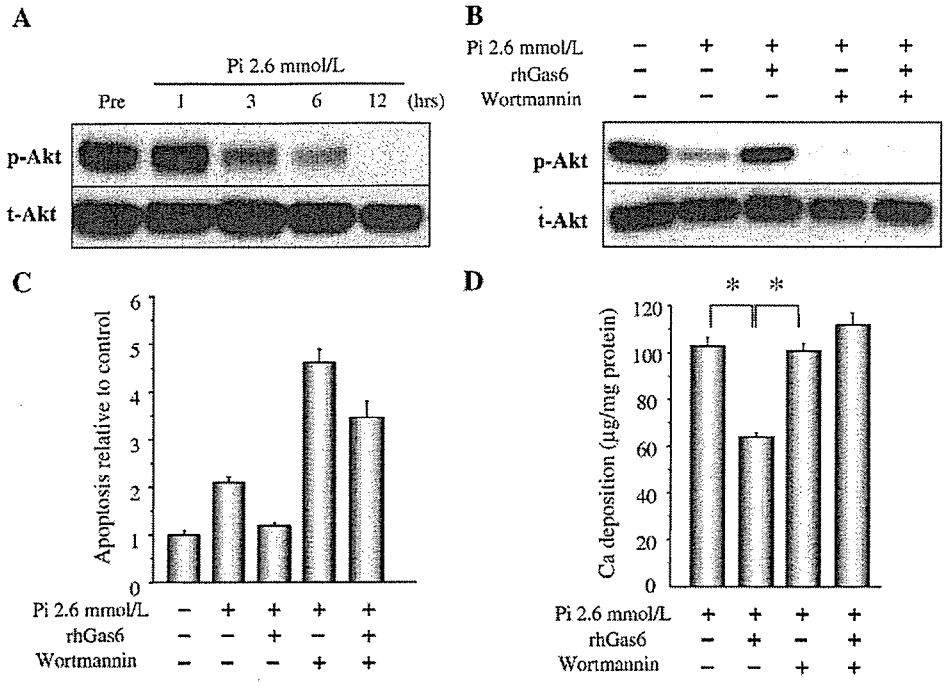

Fig. 3. Pi decreases Akt phosphorylation, and wortmannin abrogates the inhibitory effect of rhGas6 on Akt phosphorylation, apoptosis and calcification. HASMC were cultured in the presence of 2.6 mM Pi for the indicated periods. Cell lysates were immunoblotted with anti-phospho-Akt (p-Akt) antibody and total Akt (t-Akt) antibody (A). HASMC were pretreated with rhGas6 (400 ng/ml), wortmannin (1 μM), or both for 1 h, and then treated with 2.6 mM Pi for 12 h. Cell lysates were immunoblotted with p-Akt and t-Akt antibody (B). After pretreatment with rhGas6 (400 ng/ml) and wortmannin (1 μM), apoptosis was induced by 2.6 mM Pi. All values are presented as mean±S.E.M. ($n=3$). *$P<0.05$ vs. 2.6 mM Pi, rhGas6 (−), wortmannin (−) by Fisher's test (C). HASMC were cultured with rhGas6 (400 ng/ml) and with or without wortmannin (1 μM) in the presence of 2.6 mM Pi for 6 days. Ca content was measured and normalized by cell protein content. All values are presented as mean±S.E.M. ($n=6$). *$P<0.05$ by Fisher's test (D).

3.5. Gas6-mediated survival pathway is the target of statins' effect on apoptosis

To investigate whether the antiapoptotic effect of statins is associated with the Gas6-mediated survival pathway, first, we examined the effect of statins on the expression of Gas6 and Axl. As shown in Fig. 5A and B, both fluvastatin and pravastatin restored the expression of Gas6 and Axl, which was downregulated by 2.6 mM Pi. Because we have shown that the Gas6-mediated survival pathway is Akt-dependent, the effect of statins on Akt phosphorylation was examined. The Pi-induced decrease in Akt phosphorylation was restored by both statins, while total Akt expression was not changed. In addition, we found that both statins stimulated phosphorylation of Bcl2 and

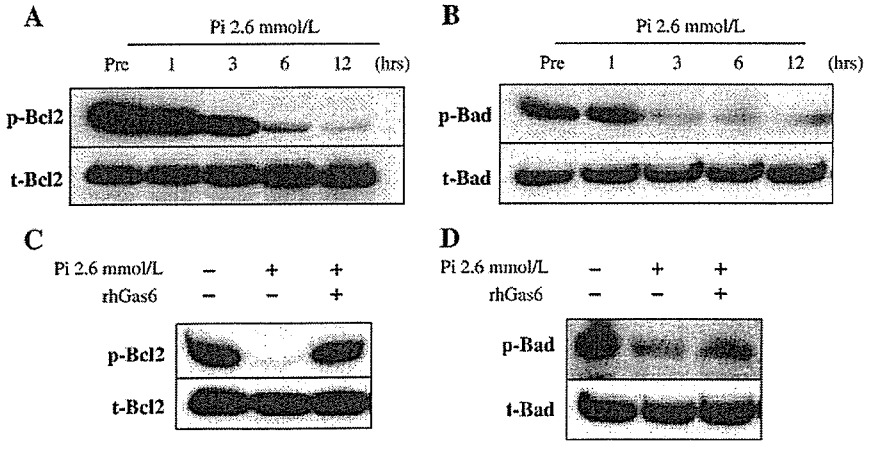

Fig. 4. RhGas6 restores Pi-induced decrease in phosphorylation of Bcl2 and Bad. HASMC were exposed to 2.6 mM Pi for the indicated periods, and cell lysates were subjected to immunoblotting with anti-phospho-Bcl2 (p-Bcl2) antibody and total Bcl2 (t-Bcl2) antibody (A), or with anti-phospho-Bad (p-Bad) antibody and total Bad (t-Bad) antibody (B). HASMC were pretreated with rhGas6 (400 ng/ml) for 1 h, and then treated with 2.6 mM Pi for 12 h. Cell lysates were subjected to immunoblotting with p-Bcl2 and t-Bcl2 antibody (C), or with p-Bad and t-Bad antibody (D).